# QUANTUM TRANSPORT IN HYBRID NANOSTRUCTURES

K. I. WYSOKIŃSKI*, T. DOMAŃSKI, B. SZUKIEWICZ

*Institute of Physics, M. Curie-Skłodowska University, 20-031 Lublin, Poland*
** E-mail: karol@tytan.umcs.lublin.pl*

GRZEGORZ MICHAŁEK, BOGDAN R. BUŁKA

*Institute of Molecular Physics, Polish Academy of Science, ul. M. Smoluchowskiego 17, 60-179 Poznań, Poland*

The study of charge, heat and spin transport in nanodevices is of theoretical and practical interest. The presence of ferromagnetic and/or superconducting electrodes adds new functionalities to the device and at the same time allows the observation of the interplay between various many body effects like e.g. Kondo effect and Andreev scattering. Here we shall consider nanosystems containing quantum dot (or a molecule) coupled to two or three external leads and analyze their local and non-local transport properties. The pairing correlations are induced in the quantum dot coupled to a superconducting lead *via* the proximity effect. For subgap voltages one observes the anomalous transport by means of direct and crossed Andreev reflections, whereas the usual single particle electronic transfer is suppressed. The interactions of electrons on the dot, leading to such phenomena as *e.g.* the Coulomb blockade severely modify the currents flowing in the system. Non-local effects in three terminal device have also been discussed and the experiments which could detect them have been proposed.

*Keywords*: quantum transport, Seebeck coefficient, Kondo effect

## 1. Introduction

The study of transport via quantum dots or single molecules is important because it is a playground for many particle theories[1] and the systems show new functionalities for future electronic applications.

The variety of novel phenomena is expected in hybrid structures in which one or more electrodes are ferromagnetic or superconducting. Such structures have been proposed as building blocks of devices with new functionalities for potentially important applications (single electron transistors, opto- and spintronic devices, etc.). They may be a source of: pure spin current,[2–4] entangled electrons[5] for quantum computing applications[6–9]





or thermoelectric heat into electricity converters, refrigerators, etc. The novel functionalities of the devices with quantum dots include their usage as building blocks of qubits[10] for quantum information purposes.

Here we shall consider the system composed of small central region, conveniently called quantum dot (QD) in the following, coupled to external electrodes. The electrodes may be normal metals or superconductors. The presence of various types of electrodes allows the study of interplay of different processes e.g. the interplay between Coulomb blockade or Kondo effect[11] and Andreev tunneling,[12] the proximity induced Andreev states in a quantum dot, etc.

It has to be stressed that with the existing experimental techniques one is able to study nanostructures under well controlled conditions. One of the best examples is the discovery and precise measurements of the single impurity Kondo effect. In nanostructures it manifests itself by increased conductance through a quantum dot coupled to two normal electrodes. Discovered in the thirties[13] of the last century as the low temperature increase of the resistance of noble metals with magnetic impurities, the effect has been named after Jun Kondo[14] who proposed its first explanation. The phenomenon has been predicted theoretically[15,16] to exist, and was later measured,[17–21] in quantum dots coupled to external metallic electrodes. In the nanostructures it has been possible to precisely measure the temperature dependence of the Kondo conductance over the full temperature range and compare the data with existing theories. The obtained agreement in the limit of linear transport i.e. weak bias voltages is remarkably good. More recent important results have been the scaling properties of the nonequlibrium Kondo effect.[22]

In the next section (2) we shall discuss some theoretical issues related to the studies of transport properties of quantum dot nanostructures. We start with modeling of such systems and description of the techniques developed to calculate transport and kinetic coefficients. We discuss there *inter alia* the necessary conditions the diffusive systems have to fulfil in order to show large values of the Seebeck coefficient. The results for the simple models of interacting quantum dot between two normal metallic electrodes are worked out exactly in the weak coupling regime in section (3). The rest of the paper is devoted to the discussion of more complicated examples including three terminal system with two normal and one superconducting lead. We end up with brief summary (Section 4).

## 2. Theoretical issues

### 2.1. *Hamiltonian of the quantum dot coupled to electrodes*

It is the standard practice to model the system by the Anderson Hamiltonian using the tunneling approximation for the coupling of the central region to the external electrodes. The Anderson Hamiltonian of the single impurity[23] can be written in the form

$$H = H_{QD} + \sum_{\alpha} H_{\alpha} + H_T \,, \tag{1}$$

where the first term describes the quantum dot, the second electrons in the leads and the third is responsible for the tunneling of electrons between the leads and the QD. In the most general case discussed here summation $\alpha$ runs over two normal (N) metals and superconductor (S). For two normal metallic electrodes we shall use notation L for left and R for right electrode.

The Hamiltonian of the single level QD reads

$$H_{QD} = \sum_{\sigma} \varepsilon_{d\sigma} d_{\sigma}^{\dagger} d_{\sigma} + U n_{\uparrow} n_{\downarrow} \,, \tag{2}$$

where $\varepsilon_{d\sigma}$ is the single-particle energy level. Its spin dependence result from the external magnetic field $\varepsilon_{d\sigma} = \varepsilon_d + g_{\sigma}\mu_B B/2$, $g_{\uparrow} = 1$, $g_{\downarrow} = -1$. Here $d_{\sigma}^{\dagger}$ ($d_{\sigma}$) denotes creation (annihilation) operator of the dot electron with spin $\sigma$, $n_{\sigma} \equiv d_{\sigma}^{\dagger} d_{\sigma}$, and $U$ is the Coulomb interaction between two electrons on the QD. It is assumed that the normal metal electrodes are non-interacting

$$H_{\alpha} = \sum_{k,\sigma} \varepsilon_{\alpha k\sigma} c_{\alpha k\sigma}^{\dagger} c_{\alpha k\sigma} \,, \tag{3}$$

where $c_{\alpha k\sigma}^{\dagger}$ ($c_{\alpha k\sigma}$) denotes creation (annihilation) of an electron with spin $\sigma$ and momentum $k$ in the electrode $\alpha = F$ or $\{L, R\}$. For a ferromagnetic (F) electrode the single particle energies depend on the spin, otherwise this dependence is neglected $\varepsilon_{\alpha k\sigma} = \varepsilon_{\alpha k}$.

If present, the third superconducting (S) electrode is described in the BCS approximation as

$$H_S = \sum_{k,\sigma} \epsilon_{Sk} c_{Sk\sigma}^{\dagger} c_{Sk\sigma} + \sum_{k} \left( \Delta c_{S-k\uparrow}^{\dagger} c_{Sk\downarrow}^{\dagger} + \Delta^* c_{Sk\downarrow} c_{S-k\uparrow} \right) \,, \tag{4}$$

with an isotropic energy gap $\Delta$. The tunneling between QD and the external leads is given by the term

$$H_T = \sum_{\alpha,k,\sigma} \left( V_{\alpha} c_{\alpha k\sigma}^{\dagger} d_{\sigma} + V_{\alpha}^* d_{\sigma}^{\dagger} c_{\alpha k\sigma} \right) \,, \tag{5}$$



where $V_{\alpha}$ is the hopping integral between QD and the $\alpha$-th lead.

If the superconducting gap $\Delta$ is the largest energy scale, so one can take the limit $\Delta \to \infty$ and effectively eliminate superconducting degrees of freedom. This amount to replacing the QD Hamiltonian $H_{QD}$ by the effective one[4,24]

$$\tilde{H}_D = \sum_{\sigma} \varepsilon_{d\sigma} d_{\sigma}^{+} d_{\sigma} + U n_{\uparrow} n_{\downarrow} - \frac{\Gamma_s}{2} d_{\uparrow}^{+} d_{\downarrow}^{+} - \frac{\Gamma_s}{2} d_{\downarrow} d_{\uparrow} \,. \tag{6}$$

The physics behind this transformation is the following. Due to the proximity effect the Cooper pair wave function 'leaks' into the quantum dot and induces pair correlation in it. This is true for finite and infinite $\Delta$. In the latter case the problem gets much simplified at the expense of neglecting all single particle tunneling processes into/from the superconductor.

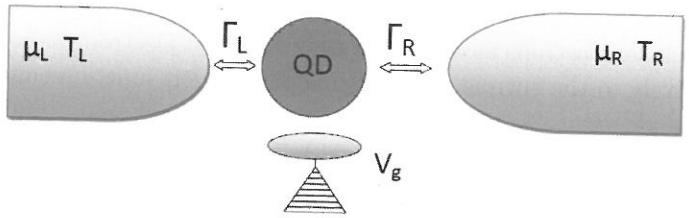


Figure 1. The system composed of quantum dot (QD) tunnel coupled to two external leads: the left characterized by the chemical potential $\mu_L$, temperature $T_L$ and the right with these parameters $\mu_R, T_R$. The effective couplings are denoted by $\Gamma_L$,$\Gamma_R$.

### 2.2. *Master equation and transition rates*

Weak and strong coupling regimes of transport are defined according to the strength of the coupling to the leads. If the couplings are weak (all $\Gamma_{\alpha}$'s being small) the charge fluctuation on the dot is suppressed and the state of the dot is well defined by the diagonal matrix elements of the density matrix. In such a case the probability $P_n$ of finding a quantum dot occupied by n -electrons (n=0,1,2 for a single level QD) completely characterizes the state of the system. The equation for time dependence of the probabilities is known as Master equation and reads[1]

$$\frac{dP_n}{dt} = -\sum_{m} W_{mn} P_n + \sum_{m} W_{nm} P_m, \tag{7}$$

where $W_{nm} \equiv W_{m\to n}$ is the transition rate from a state $m$ to $n$. The rates are typically calculated with help of Fermi golden rule and depend on the parameters of the leads, the quantum dot and the couplings $(T_L, T_R, \mu_L, \mu_R, \varepsilon_d, U, \Gamma_L, \Gamma_R)$. We are interested in the stationary state, i.e. when the average current in the nanostructure does not depend on time. The stationarity condition $\frac{dP_n}{dt} = 0$ leads to the system of equations for the probabilities

$$0 = -\sum_m W_{mn}P_n + \sum_m W_{nm}P_m, \tag{8}$$

which is solved together with the probability normalization condition $\sum_n P_n = 1$.

For the simplest case with one electron transfers as described by tunneling Hamiltonian (5) the electrons move one by one from or to the quantum dot. The possible states of the single level dot $n$ uniquely depend on the number of electrons on it $n = 0, 1, 2$. The transitions change this number by 1. Consider electrons moving onto a dot from left electrode as contributing positively to the current. The current *via* the left junction can thus be calculated as

$$I_L = -e\sum_n \left(W^L_{n\to n+1} - W^L_{n+1\to n}\right) P_n, \tag{9}$$

where $-e$ is the electron charge. The second term in brackets describes process in the L junction in which the quantum dot state with $n+1$ electrons changes to the state with $n$ electrons. It describes electron hopping from the dot to the left lead thus the minus sign. Similarly one calculates the currents across the right junction. Charge conservation implies $I_L + I_R = 0$.

The transition rates $W^L_{mn}$, $W^R_{mn}$, both contributing to $W_{mn} = W^L_{mn} + W^R_{mn}$, are calculated from the Fermi golden rule[25,26]

$$W^L_{mn} = \frac{2\pi}{\hbar}\sum_{i_n, f_m} |< f_m|H_T|i_n >|^2 W_{i_n}\delta(E_{i_n} - E_{f_m}). \tag{10}$$

Symbols $E_n(E_m)$ denote total energies of the system before and after tunneling process. Summation goes over those initial states $i_n$ and final states $f_m$ of the system which result in the states $n$ and $m$. The initial configurations are weighted by the thermal distribution function $W_{i_n}$. They lead to the Fermi distribution function $f_L(\varepsilon) = 1/(\exp((\varepsilon - \mu_L)/k_B T_L) + 1)$ for a process in which an electron tunnels onto the dot. For the inverse process of tunneling from the dot to left lead the probability $(1 - f_L(\varepsilon))$ of having empty state at the energy $\varepsilon$ in the lead L enters the calculated rate.



Let us calculate the rate $W^L_{10}$ for a model system at hand. To this end we take the initial states of the whole system as a product $|i_n >= |0\rangle_d |FS >_L$ which means no electrons on the dot and the full Fermi surface of states in the left electrode. The first term in the $H_T$ part of the Hamiltonian (5) does not contribute as $d_\sigma|0\rangle_d = 0$. The total initial energy of the system is denoted by $E_{i_n} = E_0$ and is a sum of single particle energies of electrons in the left lead. The second term in tunneling Hamiltonian $V^*_\alpha d^\dagger_\sigma c_{\alpha k\sigma}$ gives nonzero contribution only if the final state $|f_m\rangle = d^\dagger_\sigma c_{\mathbf{k}}|i_n\rangle$

$$W^L_{10} = \frac{2\pi}{\hbar}\sum_{\mathbf{k},\sigma} |\langle i_n|c^\dagger_{\mathbf{k}\sigma} H_T|i_n\rangle|^2 W_{\mathbf{k}\sigma}\delta(E_0 - (E_0 + \varepsilon_d - \varepsilon_{\mathbf{k}})). \tag{11}$$

The summation over the initial states of the system runs over $\mathbf{k}$ vectors and spins $\sigma$ of the left leads electrons. There is only single final state defined by $\delta(\varepsilon_d - \varepsilon_{\mathbf{k}})$. Introducing the Hamiltonian (5) into Eq. (11) one gets

$$W^L_{10} = \frac{2\pi}{\hbar}\sum_{\mathbf{k}\sigma} |V^L_{\mathbf{k}\sigma}|^2 \sum_{\mathbf{k}'\neq\mathbf{k}} \langle \mathbf{k}'\sigma|c^\dagger_{\mathbf{k}'\sigma} c_{\mathbf{k}'\sigma}|\mathbf{k}\sigma\rangle|^2 W_{\mathbf{k}'\sigma}\langle 0_d|d_\sigma d^\dagger_\sigma|0_d\rangle\delta(\varepsilon_{\mathbf{k}} - \varepsilon_d). \tag{12}$$

Noting that ${}_d\langle 0|d_\sigma d^\dagger_\sigma|0\rangle_d = 1$ and

$$f_L(\varepsilon_{\mathbf{k}}) = \sum_{\mathbf{k}'\neq\mathbf{k}'} \langle \mathbf{k}'\sigma|c^\dagger_{\mathbf{k}'\sigma} c_{\mathbf{k}'\sigma}|\mathbf{k}\sigma\rangle|^2 W_{\mathbf{k}'\sigma} \tag{13}$$

one gets

$$W^L_{10} = \frac{2\pi}{\hbar}\sum_{\mathbf{k}\sigma} |V^L_{\mathbf{k}\sigma}|^2 \delta(\varepsilon_{\mathbf{k}} - \varepsilon_d) f_L(\varepsilon_{\mathbf{k}}). \tag{14}$$

Changing the summation over $\mathbf{k}$ in the last equation into the integration over energy and assuming that the effective coupling

$$\Gamma_L = 2\pi\sum_{\mathbf{k}\sigma} |V^L_{\mathbf{k}\sigma}|^2 \delta(\epsilon - \varepsilon_{\mathbf{k}}) \tag{15}$$

does not depend on energy $\epsilon$ one finally gets $W^L_{10} = \frac{1}{\hbar}\Gamma_L f_L(\varepsilon_d)$. In a similar way one calculates all other transition rates. After solving master equations for the probabilities the current in each of the electrodes is calculated.

It is important to stress that the Coulomb interactions are treated in an exact way in the master equation approach. Moreover, having all expressions for the transition rates and currents in an analytic form it is a matter of simple calculation to find closed expressions for the linear kinetic coefficients. The examples of such calculations will be quoted in section (3.1) for two situations.

### 2.3. *Calculation of the currents*

The Landauer-Büttiker approach uses the scattering formalism of quantum mechanics. The idea is to calculate the transmission coefficient $T(E)$ *via* an obstacle in one dimensional (1d) system. In one dimension the wave vector $\mathbf{k}$ has a single component and we denote it simply by $k$ in the following. The calculation of the current in this case is particularly simple. Consider an electron of charge $-e$, wave vector $k$ and velocity $v(k)$ to the left of the scattering center. Approaching the scattering center (an obstacle) electron will be partially back-reflected and partially transmitted with the probability $T(\varepsilon(k))$. It is a matter of simple quantum mechanical calculations to find both reflection and transmission coefficients.

The electrical current carried by the electron moving to the right is given by summing $-ev(k)$ over all wave vectors and spins and taking into account the transmission probability $T(\varepsilon(k))$ and the probability that the state of energy $\varepsilon(k)$ is occupied

$$I_L = -e\sum_{k\sigma} v(k)T(\varepsilon(k))f_L(\varepsilon(k)). \tag{16}$$

The current flowing from the right is calculated in a similar way taking into account that to the right of the scattering center the distribution function is $f_R(\varepsilon(k))$. Total current is the difference between left and right terms. Landauer-Büttiker expressions for the charge and heat currents read[1,25]

$$I = -\frac{2e}{h}\int d\varepsilon T(\varepsilon)[f_L(\varepsilon) - f_R(\varepsilon)]$$
$$I_Q = \frac{2}{h}\int d\varepsilon(\varepsilon-\mu)T(\varepsilon)[f_L(\varepsilon) - f_R(\varepsilon)]. \tag{17}$$

The factor 2 takes spin degree of freedom into account. To obtain equation (17) it is enough to notice that in one dimension the transition from summation over wave vectors to integration over energy is simple because the density of states $\partial k/\partial\varepsilon(k)$ up to a constant equals the inverse of the velocity $v(k) = (1/\hbar)(\partial\varepsilon(k)/\partial k)$ and both these terms cancel in Equation (16). This cancellation is a property of one dimensional system.

Once the energy dependent transmission coefficient is known it is an easy task to calculate the currents and kinetic coefficients. At zero temperature and for energy and spin independent transmission $T(E) = T_0$ one gets $I = -(2e/h)T_0(\mu_L - \mu_R) = (2e^2/h)T_0V$. Here $V$ is the voltage bias. The conductance is thus given by $G = (2e^2/h)T_0$. For a system with N perfectly conducting channels $T_0 = N$ the conductance is found to be quantized in agreement with experiments.[27]



### 2.4. *Kinetic coefficients in the linear regime*

We are interested in transport properties of the structure shown in Fig. 1. Application of the voltage between L and R electrode of the structure results in the flow of charge current. Surely each electron tunneling between the leads and the dot carries not only charge but also energy and spin. It means that in general one has to consider charge $I$, spin $I_s$ and heat $I_Q$ flow. In the linear limit charge and heat currents are usually written in terms of thermodynamic forces $X_1 = (\mu_L - \mu_R)/T$ and $X_2 = (T_L - T_R)/T^2 \approx \delta T/T^2$ as

$$I = I_1 = L_{11}X_1 + L_{12}X_2$$
$$I_Q = I_2 = L_{21}X_1 + L_{22}X_2. \tag{18}$$

If the forces are chosen to give positive entropy ($\mathcal{S}$) production

$$\frac{\partial\mathcal{S}}{\partial t} = \sum_i I_iX_i > 0, \tag{19}$$

then the Onsager symmetry relations are fulfilled $L_{12}(\mathbf{B}) = L_{21}(-\mathbf{B})$, where $\mathbf{B}$ denotes the external magnetic field. Phenomenological transport coefficients are related to matrix elements of the matrix $\mathbf{L}$. The conductance G is given by $G = (e^2/T)L_{11}$, thermopower $S = -(k_B/eT)(L_{12}/L_{11})$ and the thermal conductance $\kappa = det(\mathbf{L})/(T^2L_{11})$. Less attention is usually paid to the fourth transport parameter which is the Peltier coefficient $\Pi$. It is defined as coefficient of proportionality between heat and charge currents flowing in the system in response to voltage bias under isothermal $\delta T = 0$ conditions

$$\Pi = \left(\frac{I_Q}{I}\right)_{\delta T=0} = \frac{L_{21}}{L_{11}}, \tag{20}$$

and is directly related to the Seebeck coefficient $S$.

The combination of transport coefficients

$$ZT = \frac{GS^2}{\kappa/T}, \tag{21}$$

known as thermoelectric figure of merit, is a single dimensionless number traditionally used for characterizing the usefulness of a given material or structure as a heat to electric power converter. This is because the theoretical estimation of the maximal efficiency $\eta_{max}$ of the material can be expressed by Carnot efficiency $\eta_C$ and the above number $ZT$ as

$$\eta_{max} = \eta_C\frac{\sqrt{ZT+1}-1}{\sqrt{ZT+1}+1}. \tag{22}$$

### 2.5. *Remarks on the thermoelectric power*

In the Fermi liquid theory electrical and thermal conductances are related to each other *via* Wiedemann-Franz ratio $\kappa/(GT)$, which for the Fermi liquids equals to the Lorenz number $L_0 = \pi^2 k_B^2/(3e^2)$, where $k_B$, $e$ are the Boltzmann constant and electric charge, respectively. This shows that the system obeying the Wiedemann-Franz law is a useful thermoelectric power generator if its Seebeck coefficient is high.

It is thus important to know what are the conditions for large values of the thermopower $S$. The general analysis of the factors favoring high values of the thermopower has been performed by Mahan and Sofo[28] who concluded that *"A delta-shaped transport distribution is found to maximize the thermoelectric properties."* We shall here give slightly less general, but still instructive arguments. To this end we write the electrical conductivity in the form

$$\sigma = \int_{-\infty}^{\infty} d\varepsilon \left(-\frac{\partial f}{\partial \varepsilon}\right) \sigma(\varepsilon). \tag{23}$$

In the Boltzmann or Kubo-Greenwood approach to conductivity the function $\sigma(\varepsilon)$ reads

$$\sigma(\varepsilon) = \sum_{\mathbf{k}} v_x(\mathbf{k}) \tau(\mathbf{k}) \delta(\varepsilon - \varepsilon_{\mathbf{k}}), \tag{24}$$

where $\tau(\mathbf{k})$ is the transport relaxation rate for electrons in state $\mathbf{k}$ and $v_x(\mathbf{k})$ is their velocity. For a simple parabolic band structure this may be written as the product of energy dependent quantities i.e.

$$\sigma(\varepsilon) = N(\varepsilon) v_x(\varepsilon) \tau(\varepsilon), \tag{25}$$

with $N(\varepsilon)$ denoting the density of states. Now it is useful to recall the famous, even though approximate, low temperature relation for the thermopower, known as Mott-Cutler (MC) formula, which gives S in term of conductivity at the Fermi energy $\sigma(\varepsilon_F)$

$$S_{MC} = -\frac{\pi^2}{3} \frac{k_B}{e} k_B T \frac{1}{\sigma(\varepsilon_F)} \left(\frac{d\sigma(\varepsilon)}{d\varepsilon}\right)_{\varepsilon_F}. \tag{26}$$

The derivation of the formula[29] bases on the low temperature Sommerfeld expansion.

Plugging the expression (25) evaluated at $\varepsilon = \varepsilon_F$ into (26) we see that for nonzero S one needs that at least one of the factors: density of states, average velocity or transport relaxation time do depend on energy in the vicinity of Fermi energy. If the resulting function strongly varies with the Fermi energy one gets the large value for S. The slopes of each of the parameters with respect to change of $\varepsilon_F$ add to give $S_{MC}$ as a sum of three terms, each of which may have different sign. It thus follows that e.g. the existence of the peak in the density of states close to the Fermi level of the material may indicate large thermopower. At the same time even if $N(\varepsilon_F)$ is constant the thermopower may still take non-zero value due to the velocity or relaxation time varying in the vicinity of Fermi energy.



In the nanostructures transport is ballistic and the resulting conductance G depends on the density of states only. This means that the slope of the density of states at the Fermi energy is the main factor determining Seebeck coefficient $S$. On the other hand one has to remember that the Mott-Cutler[29] formula is not exact expression for $S$.

## 3. Results

Here we present results for a few simple cases. We start with a quantum dot system between two normal metal electrodes. This model has been proposed as a system with very large thermoelectric figure of merit.[30] The details related to the currents flowing in the system and Seebeck coefficient are discussed in some detail and compared to the molecular system which supports attractive interactions on the dot. More general system with three external terminals has been discussed in Section 3.2. The system, shown in the Fig. 4 consists of a quantum dot and three terminals, one of them being a BCS superconductor in the large $\Delta$ limit.

### 3.1. *Two terminal transport - normal electrodes*

Here we shall discuss conductances and thermopowers in the geometry of Fig. 1 assuming first that the central region is just an interacting quantum dot. We calculate the charge and heat currents using master equations.

In the linear response regime $T_L - T_R = \delta T \to 0$ and $\mu_L - \mu_R = -eV \to 0$ the Fermi functions are expanded in power series of $\delta T$ and $eV$. Assuming symmetric temperature and bias distribution $\mu_{L(R)} = \mu \pm eV/2$ and $T_{L(R)} = T \pm \delta T$ we find transport coefficients $L_{ij}$ and the conductance and thermopower defined earlier. This leads to the following expressions[30]

for the conductance $G$ and Seebeck coefficient $S$

$$G = \frac{2e^2}{h}\frac{2\Gamma_L\Gamma_R}{\Gamma_L+\Gamma_R}\frac{e^{\frac{\varepsilon_d+U}{k_BT}}[1+e^{\frac{\varepsilon_d}{k_BT}}(e^{\frac{\varepsilon_d+U}{k_BT}}+2)]}{k_BT(e^{\frac{\varepsilon_d}{k_BT}}+1)(e^{\frac{\varepsilon_d+U}{k_BT}}+1)[1+e^{\frac{\varepsilon_d+U}{k_BT}}(e^{\frac{\varepsilon_d}{k_BT}}+2)]} \quad (27)$$

$$S = -\frac{k_B}{e}\frac{\frac{\varepsilon_d}{k_BT}[1+e^{\frac{\varepsilon_d}{k_BT}}(2+e^{\frac{\varepsilon_d+U}{k_BT}})]+\frac{U}{k_BT}(e^{\frac{\varepsilon_d}{k_BT}}+1)}{1+e^{\frac{\varepsilon_d}{k_BT}}(e^{\frac{\varepsilon_d+U}{k_BT}}+2)}. \quad (28)$$

It is interesting to note that the conductance of the system is a function of $\varepsilon_d/k_BT$ and $U/k_BT$ and is given by the universal function $G(\varepsilon_d,U,T) = F_G(\varepsilon_d/T,U/T)/T$. In a similar way thermopower is given by other universal function of the same variables scaled by temperature $S(\varepsilon_d,U,T) = F_S(\varepsilon_d/T,U/T)$.

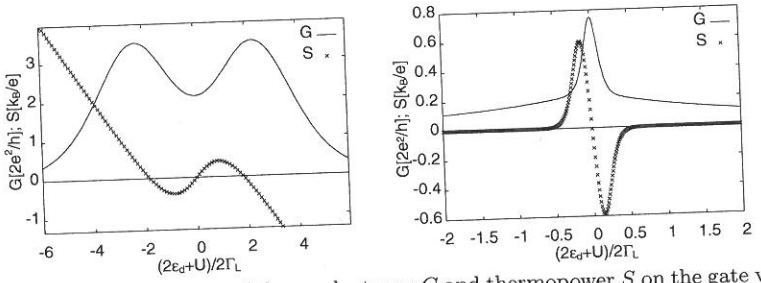


Figure 2. The dependence of the conductance $G$ and thermopower $S$ on the gate voltage measured with respect to the degenarcy point for the symmetrically coupled quantum dot $\Gamma_R = \Gamma_L = 1$ for temperature $T = 0.05\Gamma_L$. Left panel illustrates results for the quantum dot with positive $U = 4\Gamma_L$. Similar dependence of the same kinetic coefficients ($G$ and $S$) for a molecular central region with effective negative $U = -4\Gamma_L$ is shown in the right panel.

If the central region consists of a molecule, there may arise interesting situation in which the effective interaction between electrons on a quantum dot is negative: $U < 0$. This is due to the coupling of electrons to vibrational degrees of freedom[31] which renormalizes hopping parameters and interaction energy $U$. The effective system - after elimination of the coupling to vibrational degrees of freedom - is the same as that for a quantum dot but with negative $U$. The physics behind its transport properties as discussed [31] in detail by Koch et al., however, is completely different. The single particle tunneling is suppressed and two particle processes dominate.

To capture these processes it is enough to perform Schrieffer-Wolf transformation. The effective tunneling Hamiltonian[31] contains terms describing direct tunneling between two electrodes and those promoting two particle



events in which two electrons are created or annihilated on the molecule at the expense of one or both electrodes

$$H_T = H_{dir,ex} + H_{pair} = \frac{1}{2}\sum_{\lambda\lambda'\mathbf{k}\mathbf{k}'\sigma} V_\lambda V^*_{\lambda'}\Big[\frac{1}{\varepsilon_{\lambda\mathbf{k}}-\varepsilon_d}c^\dagger_{\lambda\mathbf{k}\sigma}c_{\lambda'\mathbf{k}'\sigma} + M(\varepsilon_{\lambda\mathbf{k}})(d^\dagger_{-\sigma}d_\sigma c^\dagger_{\lambda\mathbf{k}\sigma}c_{\lambda'\mathbf{k}'-\sigma} - c^\dagger_{\lambda\mathbf{k}\sigma}c_{\lambda'\mathbf{k}'\sigma}n_{d\bar{\sigma}}) + H.c.\Big] + \sum_{\lambda\lambda'\mathbf{k}\mathbf{k}'}\Big[V_\lambda V^*_{\lambda'}M(\varepsilon_{\lambda\mathbf{k}})d_\uparrow d_\downarrow c^\dagger_{\lambda'\mathbf{k}'\downarrow}c^\dagger_{\lambda\mathbf{k}\uparrow} + H.c.\Big], \quad (29)$$

where $M(\varepsilon) = [\varepsilon-\varepsilon_d]^{-1} - [\varepsilon-\varepsilon_d-U]^{-1}$.

Treating the system as weakly coupled and using master equation approach one derives expressions for conductance[31] $G_M$ and thermopower[32] $S_M$ of such a molecular system for symmetric couplings $\Gamma_L = \Gamma_R = \Gamma$. They read[31,32]

$$G_M = \frac{2e^2}{h}\Gamma_L\Gamma_R\Big[M^2(0)\frac{\beta x}{2\sinh\beta x} + \frac{f(-x)}{\varepsilon_d^2} + \frac{f(x)}{(\varepsilon_d+U)^2}\Big] \quad (30)$$

$$S_M = -\frac{k_B}{e}\frac{M^2(0)\beta^2x^2/4\sinh\beta x}{G_M}. \quad (31)$$

The parameter $x = 2\epsilon_d + U$ denotes distance from the degeneracy point, $\beta = 1/k_BT$.

Figure 2 shows the dependence of the conductance and thermopower of the two studied systems on the gate voltage. In both panels we measure the energies in unit of $\Gamma_L$ and from the particle-hole symmetry point $2\varepsilon_d+U = 0$. The Seebeck coefficient of both systems vanish at that point as a result of symmetry. On the other hand conductance of the system with positive $U$ has a minimum, while that of negative $U$ is maximal in that point. For positive $U$ the single particle transitions go *via* $\varepsilon_d$ and $\varepsilon_d+U$ levels. At these points conductance has maxima and a minimum in between. On the other hand close to the degeneracy point $x = 0$ the transport through a molecular system (negative $U$) is dominated by the pair tunneling processes.[31] The peak of width $T$ is centered at $x = 0$. It is accompanied by the broad contribution from single particle co-tunneling processes. As a result $G$ and $S$ depend not only on the ratios $U/k_BT$ and $\varepsilon_d/k_BT$ but also on $U$ and $\varepsilon_d$. This leads to non-trivial $\varepsilon$ dependence of conductance and more importantly Seebeck coefficient. At low temperatures the pair tunneling shows up as a relatively narrow peak on the broad background. As a result thermopower is positive for negative values of $x$ as it is evident from Mott-Cutler formula (26), vanishes at the particle hole symmetric point and changes sign for

$x > 0$ in agreement with change of the slope of the conductance *vs.* $\varepsilon_d$. At some values of $|x|$ the slope is maximal and this leads to the maximal value of $S$. For larger $|x|$ the slope gets smaller and thermopower vanishes The width of the pair contribution to $G$ increases with temperature and its slope monotonically changes.

Applying magnetic field splits the energy levels of a quantum dot and may lead to the spin dependent currents $I_\uparrow$ and $I_\downarrow$ and the spin dependent conductances $G_\uparrow$, $G_\downarrow$. The probability that the spin down electron occupies an empty dot is in the presence of the magnetic field much larger then for spin up electron. As a result the conductance of spin up electrons currents flowing *via* resonant level $\varepsilon_{d\downarrow}$ is small and *vice versa* for second electron on the dot with opposite spin.[33] Its resonance level with large probability equals $\varepsilon_\downarrow + U$ and with much smaller probability $\varepsilon_\uparrow + U$. This is reflected in different amplitudes of the conductance. The gate voltage dependence of the conductances $G_\uparrow$ and $G_\downarrow$ is shown in the Fig. 3.

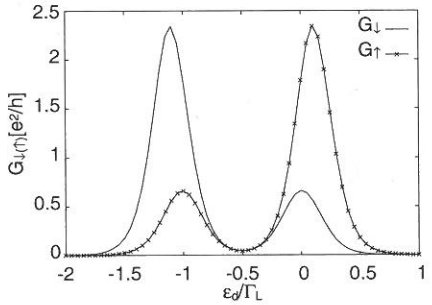


Figure 3. The gate dependence of the conductances $G_\uparrow$ and $G_\downarrow$ for the symmetrically coupled quantum dot $\Gamma_R = \Gamma_L = 1$ for the temperature $T = 0.1\Gamma_L$ and magnetic field $\mu_B B = 0.2\Gamma_L$. Note the small spin up conductance around the resonant level $\varepsilon_\downarrow$. For these values of the gate voltage the probability of finding single spin up electron on the quantum dot is much lower then that for spin down.

### 3.2. *Three terminal transport - hybrid structure*

As mentioned in the Introduction the hybrid devices consisting of normal, magnetic and/or superconducting electrodes have been found to show new functionalities[34] not encountered in simple systems. Such structures include *inter alia* planar systems [7,8,35,36] or devices containing quantum dots. The later systems consisting of a quantum dot tunnel coupled to two or more



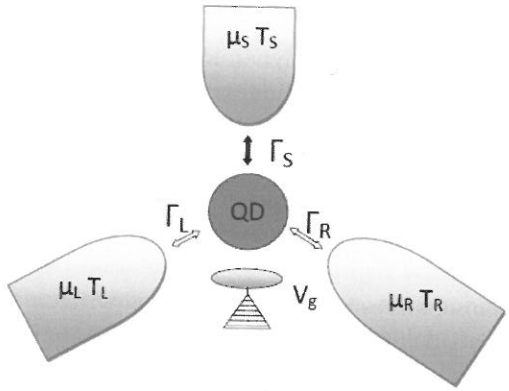


Figure 4. The system composed of quantum dot (QD) tunnel coupled to three external leads: the left characterized by the chemical potential $\mu_L$, temperature $T_L$ and the right with these parameters $\mu_R, T_R$ as previously and third electrode is a BCS superconductor. The effective couplings are denoted by $\Gamma_L$,$\Gamma_R$ and $\Gamma_S$.

electrodes, one of which is superconducting have been intensively studied theoretically[24,37–55] and experimentally.[56–64] The research on the transport through quantum dots in systems with superconducting electrodes has been reviewed[65] recently.

In three terminal setup shown in the Fig. 4 the currents fulfill Kirchhoff's law $I_L + I_R + I_S = 0$, which reflect conservation of charge. The conservation of energy requires similar equation for the heat currents $I_L^Q + I_R^Q + I_S^Q = 0$. Thus we have two independent fluxes. If we assume that the S electrode is a reference one with $T_S = T$ and $\mu_S = \mu$, while $T_{L(R)} = T + \delta T_{L(R)}$ and $\mu_{L(R)} = \mu + eV_{L(R)}$ then the phenomenological equations (18) may conveniently be generalized for the currents $I_1, I_2$ and $I_1^Q, I_2^Q$ flowing in L and R electrodes. The third current is calculated from conservation law.

For the numerical examples shown below we have used the model[66] analyzed earlier by Michałek et al. The model describes the quantum dot in contact with three electrodes: one superconducting and two normal. The superconducting electrode has a BCS like gap parameter $\Delta$, constant over the Fermi surface. It has also been assumed that $\Delta$ is the highest energy scale in the problem. Accordingly the limit $\Delta \to \infty$ has been taken. This approximation is suitable for the studies of sub-gap transport. In that limit the coupling between the superconducting electrode and the quantum dot $\Gamma_S$ plays the role of effective order parameter induced on the quantum dot *via* proximity effect.

### 3.2.1. *Symmetries of linear response coefficients*

It is convenient to use the thermodynamic forces in a close analogy to $X_1$ and $X_2$ introduced in the two terminal transport. In order not to confuse voltage and thermal bias we change the notation[67] and write $\frac{eV_L}{T} = X_1^V$, $\frac{\delta T_L}{T^2} = X_1^T$, $\frac{eV_R}{T} = X_2^V$ and $\frac{\delta T_R}{T^2} = X_2^T$. Accordingly we denote the currents flowing in the left and right electrodes as $I_L^e = I_1$, $I_L^Q = I_1^Q$, $I_R^e = I_2$ and $I_R^Q = I_2^Q$.

In the linear response regime the general relation between the currents $\vec{I}$ and thermodynamic forces inducing them $\vec{X}$ is written as

$$\begin{pmatrix} I_1 \\ I_1^Q \\ I_2 \\ I_2^Q \end{pmatrix} = \mathbf{L}\vec{X} = \begin{pmatrix} L_{11}, L_{12}, L_{13}, L_{14} \\ L_{21}, L_{22}, L_{23}, L_{24} \\ L_{31}, L_{32}, L_{33}, L_{34} \\ L_{41}, L_{42}, L_{43}, L_{44} \end{pmatrix} \begin{pmatrix} X_1^V \\ X_1^T \\ X_2^V \\ X_2^T \end{pmatrix}. \tag{32}$$

This equation is the basis of general analysis of the three terminal system. In the absence of magnetic field and other time reversal symmetry breaking factors the matrix of kinetic coefficients is symmetric $L_{ij} = L_{ji}$. The currents in the system and elements of the matrix $L_{ij}$ have been calculated with help of non-equilibrium Green function technique.[26]

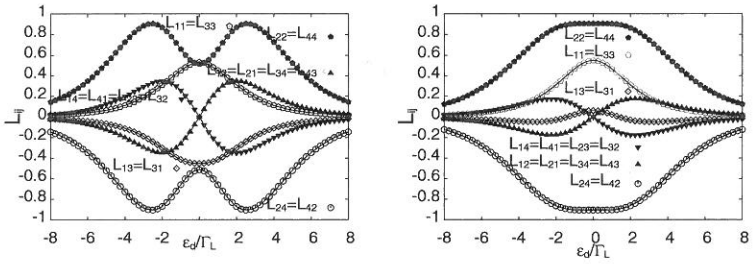


Figure 5. The matrix of kinetic coefficients plotted *vs.* on-dot energy level $\varepsilon_d$ for the symmetrically coupled quantum dot $\Gamma_R = \Gamma_L = 1$ and for weak $\Gamma_S = 0.5\Gamma_L$ coupling to the superconducting lead (left panel) and strong coupling $\Gamma_S = 5\Gamma_L$ (right panel) . Only 6 coefficients out of 16 are independent in the linear regime.

The dependence of all the kinetic coefficients $L_{ij}$ on the position of the on-dot energy level $\varepsilon_d$ (or gate bias) for symmetric coupling to the left and right electrode $\Gamma_L = \Gamma_R$ is shown in Fig. 5 for weak $\Gamma_S = 0.5\Gamma_L$ (left panel) and strong $\Gamma_S = 5\Gamma_L$ coupling to the superconducting electrode



(right panel). The matrix, in agreement with the Onsager relations, is symmetric $L_{ij} = L_{ji}$ as the time reversal symmetry is preserved. Note the change of the shape of the curves $L_{13} = L_{31}$ in the strong coupling limit.

### 3.2.2. *Non-local effects - induced voltages and temperatures*

In three-terminal system the current effectively flows in two branches. This allows study of local and non-local effects, as e.g. the current flowing in the right branch of the system in response to the voltage bias in the left one. One defines the floating electrodes as that in which the current does not flow. Here we shall consider more general definition. We require that in the floating electrode, assumed to be the right (R) one both charge and heat currents vanish i.e. $I_R^e = 0$ and $I_R^Q = 0$. In the linear regime this allows to write the condition for the induced changes of the chemical potential $\delta\mu_R = eV_R$ and temperature $\delta T_R$ as

$$\begin{pmatrix} I_L^e \\ I_L^Q \\ 0 \\ 0 \end{pmatrix} = \begin{pmatrix} L_{11}, L_{12}, L_{13}, L_{14} \\ L_{21}, L_{22}, L_{23}, L_{24} \\ L_{31}, L_{32}, L_{33}, L_{34} \\ L_{41}, L_{42}, L_{43}, L_{44} \end{pmatrix} \begin{pmatrix} \frac{eV_L}{T} \\ \frac{\delta T_L}{T^2} \\ \frac{eV_R}{T} \\ \frac{\delta T_R}{T^2} \end{pmatrix}. \tag{33}$$

The current flowing in one of the branches of three terminal system may induce voltages and temperature gradients in other branch. This is a non-local effect, which we analyze here in some detail.

Solution of the system of equations (33) reads

$$\begin{pmatrix} \frac{eV_L}{T} \\ \frac{\delta T_L}{T^2} \\ \frac{eV_R}{T} \\ \frac{\delta T_R}{T^2} \end{pmatrix} = \begin{pmatrix} L_{11}, L_{12}, L_{13}, L_{14} \\ L_{21}, L_{22}, L_{23}, L_{24} \\ L_{31}, L_{32}, L_{33}, L_{34} \\ L_{41}, L_{42}, L_{43}, L_{44} \end{pmatrix}^{-1} \begin{pmatrix} I_L^e \\ I_L^Q \\ 0 \\ 0 \end{pmatrix}. \tag{34}$$

This allows calculation of $V_R$ and $\delta T_R$ for arbitrary $V_L$ and $\delta T_L$. After an easy algebra one finds the induced voltages and changes in the temperature of the right electrode

$$\begin{pmatrix} \frac{eV_R}{T} \\ \frac{\delta T_R}{T^2} \end{pmatrix} = -\begin{pmatrix} L_{33}, L_{34} \\ L_{43}, L_{44} \end{pmatrix}^{-1} \begin{pmatrix} L_{31}, L_{32} \\ L_{41}, L_{42} \end{pmatrix} \begin{pmatrix} \frac{eV_L}{T} \\ \frac{\delta T_L}{T^2} \end{pmatrix}, \tag{35}$$

and from equation (34) the corresponding currents in the left electrode

$$\begin{pmatrix} \tilde{I}_L^e \\ \tilde{I}_L^Q \end{pmatrix} = \left[ \begin{pmatrix} L_{11}, L_{12} \\ L_{21}, L_{22} \end{pmatrix} - \begin{pmatrix} L_{13}, L_{14} \\ L_{23}, L_{24} \end{pmatrix} \begin{pmatrix} L_{33}, L_{34} \\ L_{43}, L_{44} \end{pmatrix}^{-1} \begin{pmatrix} L_{31}, L_{32} \\ L_{41}, L_{42} \end{pmatrix} \right] \begin{pmatrix} \frac{eV_L}{T} \\ \frac{\delta T_L}{T^2} \end{pmatrix}. \tag{36}$$

The second term in square brackets comes from the feedback voltages and temperature gradients and is responsible for the modification of the currents with respect to those obtained from the equation (32) with both electrodes biased. The modifications are the direct consequence of the floating character of the $R$ electrode.

The amplitude and sign of the voltages induced in the floating electrode depend on the gate voltage $\varepsilon_d$ and the strength of the coupling to the superconducting electrode $\Gamma_S$. Consider first the dot with $\varepsilon_d$ close to 0 and large value of $\Gamma_S$. Application of voltage bias to the left electrode $V_L$ induces different processes. First of them is the tunneling of an electron from the left Fermi level of left electrode onto the quantum dot. The electron on the dot may then tunnel onto the right lead. This process slightly increases the voltage on the right electrode $V_R$. Electron residing on dot can not tunnel directly onto superconducting electrode as there are no states available at the Fermi energy. But it may attract another electron with different spin from one of the leads, form a Cooper pair and tunnel into the superconductor. This process (known as direct Andreev reflection) does not change the voltage bias of the right electrode $V_R$. However, the process in which electron on the dot attracts another electron from the right electrode, forms a Cooper pair and tunnels into the superconductor decreases the voltage $V_R$. For relatively large $\Gamma_S$ the crossed process may strongly renormalize voltage $V_R$ and change its sign with respect to $V_L$. The last process is known as crossed Andreev reflection. The importance of crossed Andreev processes increases with $\Gamma_S$. The tunneling of electrons between two normal electrodes always competes with Andreev reflections. As a result the curves in the left panel of the Fig. 6 show a minimum close to $\varepsilon_d = 0$ for all values of $\Gamma_S$. Similar arguments apply for other value of $\varepsilon_d$. The tunneling electrons carry not only charge but also energy. In the process they modify the occupation probabilities and electron energy in the electrodes. The resulting change of the temperature in the right electrode due to bias voltage $V_L$ is shown in the right panel of the figure. In the linear response all currents in the system are vanishingly small. However



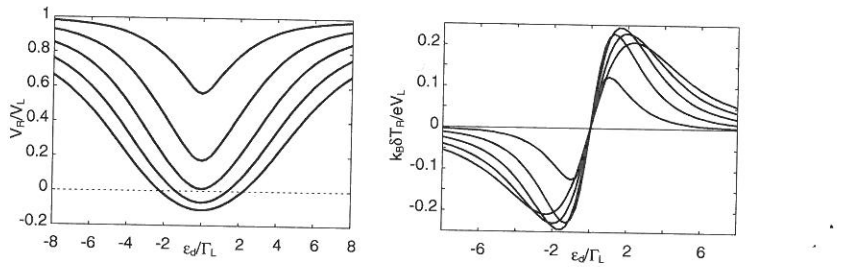


Figure 6. The ratio of the voltage $V_R$ induced in the right electrode to the voltage applied to the left one $V_L$ (left panel) and the ratio of the induced temperature change $k_B\delta T_R/eV_L$ (right panel) plotted *vs.* on-dot energy level $\varepsilon_d$ for the non-interacting $U = 0$, symmetrically coupled $\Gamma_R = \Gamma_L = 1$ quantum dot. Various curves in the left panel corrrespond to $\Gamma_S = 1, 2, 3, 4, 5\Gamma_L$ from top to bottom curve, while those in the right panel correspond to the same order around $\varepsilon_d/\Gamma_L = -6$.

the current in the left electrode of the system with floating right electrode may be written as

$$\begin{pmatrix} \tilde{I}_L^e \\ \tilde{I}_L^Q \end{pmatrix} = \begin{pmatrix} L_{11}^{eff}, L_{12}^{eff} \\ L_{21}^{eff}, L_{22}^{eff} \end{pmatrix} \begin{pmatrix} \frac{eV_L}{T} \\ \frac{\delta T_L}{T^2} \end{pmatrix}, \tag{37}$$

and differs from $I_L^e$ defined in equation (32) valid for both electrodes biased. The effective kinetic coefficients $L_{ij}^{eff}$ describe the charge and heat currents flowing in the left branch of the hybrid system with the right electrode grounded. They differ from the coefficients $L_{ij}$ for $i, j = 1, 2$ defined in (32) due to the feedback effects. The local linear conductance is given by $(e^2/h)L_{11}$. On the other hand the effective conductance related to the charge flow in the left electrode when the right one is grounded is given by $L_{11}^{eff}$; $G^{eff} = (e^2/h)L_{11}^{eff}$ with

$$L_{11}^{eff} = L_{11} - \frac{(L_{13}L_{44} - L_{14}L_{43})L_{31} + (L_{14}L_{33} - L_{13}L_{34})L_{41}}{L_{33}L_{44} - L_{34}L_{43}}. \tag{38}$$

Accordingly we may define the local Seebeck coefficients $S$ and $S^{eff}$ by requiring vanishing of the respective currents

$$S = -\left(\frac{V_L}{\delta T_L}\right)_{I_L^e=0} = \frac{L_{12}}{TL_{11}} \tag{39}$$

$$S^{eff} = -\left(\frac{V_L}{\delta T_L}\right)_{\tilde{I}_L^e=0} = \frac{L_{12}^{eff}}{TL_{11}^{eff}}. \tag{40}$$

In Fig. 7 the comparisons of both conductances and thermopowers have been presented. The smaller values of the effective conductance $G^{eff}$ and decreased amplitude of the thermoelectric power $S^{eff}$ for all positions of the

on-dot energy level $\varepsilon_d$ are related to the modifications of kinetic coefficients (like that in the equation (38)) due to back-action of the floating electrode. Despite the decrease of the effective conductance and thermopower, the

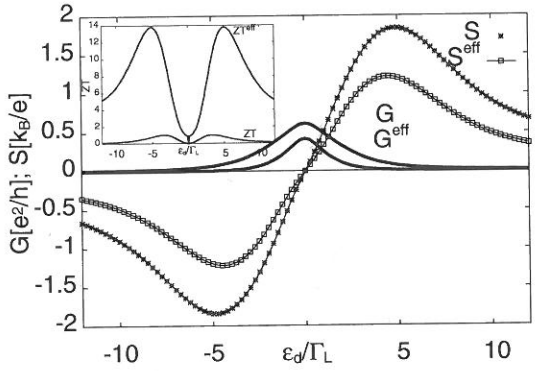


Figure 7. The conductances $G$ and $G^{eff}$ (thick lines) and thermopowers $S$ and $S^{eff}$ (lines with symbols) *vs.* on-dot energy level $\varepsilon_d$ for the symmetrically coupled quantum dot $\Gamma_R = \Gamma_S = 1\Gamma_L$ and for $T/\Gamma_L = 1$. The insert shows the thermoelectric figures of merit for the two cases. An order of magnitude increase of $ZT^{eff}$ is directly related to strongly reduced effective thermal conductivity.

thermoelectric figure of merit defined with effective coefficients takes on much large values than that of the original system. This behavior, shown in the inset to the Fig. 7, is traced back to the strong reduction of the effective thermal conductance $\kappa$ in the system with one floating electrode.

## 4. Summary and conclusions

We have reviewed a number of issues relevant in the studies of transport properties of nanostructures containing quantum dots. The necessary conditions which the systems have to fulfill in order to show non-zero value of the Seebeck coefficient have been discussed. In the weak tunneling limit master equation technique is adequate and it provides exact treatment of the Coulomb on-dot interaction $U$. Two terminal quantum dot with positive $U$ is characterized by very large figure of merit[30] ZT. On the other hand this parameter for a molecule characterized by negative effective $U$ is rather small[32] despite the large value of the thermoelectric power S. The dependence of $G$ and $S$ of two models on the gate voltage is completely different due to the fact that transport is dominated by single particle properties in



the positive $U$ case, while two-particle transitions play the most important role in the model with attractive interaction on the molecule.

Three terminal system consisting of a quantum dot tunnel coupled to two normal and one superconducting electrode has been studied using Keldysh non-equilibrium Green function technique. In the linear regime the transport coefficients $L_{ij}$ fulfill Onsager symmetry relations. The existence of the feedback effects in the system with one floating electrode is an important result of our preliminary analysis of charge and heat transport presented in Section 3.2.2. The feedback effect suppresses effective transport coefficients (see Fig. 7) due to self-consistent modification of the thermodynamic forces. The effect which is present in any multi-terminal setup remains to be detected experimentally. One possible way of its detection would be the precise measurements of the temperature changes in both normal electrodes, when one of them is subject to the external voltage. The effect should also be observable in three terminal system with all normal electrodes. The predicted numerical changes of $V_R/V_L$ and $\delta T_R/V_L$ (Fig. (6)), however, would be different.

## Acknowledgments

This work has been partially supported by the NCN grants DEC-2011/01/B/ST3/04428 and DEC-2012/05/B/ST3/03208.

## References

1. Y.V. Nazarov and Y.M. Blanter, *Quantum transport: introduction to nanoscience* (Cambridge University Press, Cambridge, 2009).
2. S. Das, S. Rao and A. Saha, *Europhys. Lett.* **81**, 67001 (2008).
3. R. Lü, H-Z Lu, X. Dai and J. Hu, *J. Phys. Condens. Matter* **21** 495304 (2009).
4. D. Futterer, M. Governale and J. Koenig, *EPL* **91**, 47004 (2010).
5. P. Recher, E.V. Sukhorukov and D. Loss, *Phys. Rev. B* **63**, 165314 (2001).
6. D. Beckmann, H. B. Weber and H. v. Löhneysen, *Phys. Rev. Lett.* **93**, 197003 (2004).
7. S. Russo, M. Kroug, T. M. Klapwijk and A. F. Morpurgo, *Phys. Rev. Lett.* **95**, 027002 (2005).
8. J. L. Webb, B. J. Hickey and G. Burnell, *Phys. Rev. B* **86**, 054525 (2012).
9. J. Wei and V. Chandrasekhar, *Nature Physics* **6**, 494 (2010).

10. D. Loss and D. DiVincenzo, *Phys. Rev. A* **57**, 120 (1998); G. Burkard, D. Loss and D. DiVincenzo, *Phys. Rev. B* **59**, 2070 (1999).
11. A. C. Hewson, *The Kondo problem to Heavy Fermions* (Cambridge University Press, Cambridge, 1993).
12. A. F. Andreev, *Zh. Eksp. Teor. Fiz.* **46**, 1823 (1964). *Sov. Phys. JETP* **19**, 1228 (1964).
13. W.J. de Haas and G.J. van den Berg, *Physica* **1**, 1115 (1934).
14. Jun Kondo, *Prog. Theor. Phys.* **32** 37 (1964).
15. L. I. Glazman and M. E. Raikh, *JETP Lett.* **47**, 452 (1988).
16. T.K. Ng, P.A. Lee, *Phys. Rev. Lett.* **61**, 1768 (1988).
17. D. Goldhaber-Gordon, H. Shtrikman, D. Mahalu, D. Abush-Maggder, U. Meirav and M. A. Kastner, *Nature* **391**, 156 (1998).
18. S.M. Cronenwett, T.H. Oosterkamp and L.P. Kouwenhoven, *Science* **281**, 540 (1998).
19. J. Schmid, J. Weis, K. Eberl and K. von Klitzing, *Physica B* **256-258**, 182 (1998); J. Schmid, J. Weis, K. Eberl and K. von Klitzing, *Phys. Rev. Lett.* **84**, 5824 (2000).
20. F. Simmel, R.H. Blick, J.P. Kotthaus, W. Wegsheider and M. Bichler, *Phys. Rev. Lett.* **83**, 804 (1999).
21. S. Sasaki, S. De Franceschi, J.M. Elzerman, W.G. van der Wiel, M. Eto, S. Tarucha and L.P. Kouwenhoven, *Nature* **405**, 764 (2000).
22. M. Grobis, I. G. Rau, R. M. Potok, H. Shtrikman, and D. Goldhaber-Gordon, *Phys. Rev. Lett.* **100**, 246601 (2008).
23. P.W. Anderson, *Phys. Rev.* **124**, 41 (1961).
24. Y. Tanaka, N. Kawakami and A. Oguri, *J. Phys. Soc. Japan* **76**, 074701 (2007) (see also **77** 098001 (1998)); *Physica E*, **40**, 1618 (2008); *Phys. Rev. B* **78** 035444 (2008); *Phys. Rev. B* **81**, 075404 (2010); Y. Yamada, Y. Tanaka, N. Kawakami, *Phys. Rev. B* **84**, 075484 (2011).
25. H. Bruus and K. Flensberg, *Many-body quantum theory in condensed matter physics*, Oxford Graduate Texts (New York: Oxford University Press, 2004), 152-183.
26. H. Haug and A.-P. Jauho, *Quantum Kinetics in Transport and Optics of Semiconductors*, (Springer Verlag, Berlin, 1996).
27. B. J. van Wees, H. van Houten, C.W. J. Beenakker, J. G.Williamson, L. P. Kouwenhoven, D. van der Marel and C. T. Foxon, *Phys. Rev. Lett.* **60**, 848 (1988).
28. G.D. Mahan and J.O. Sofo, *Proc. Natl. Acad. Sci.* **93**, 7436 (1996).
29. M. Cutler, N.F. Mott, *Phys. Rev.* **181**, 1336 (1969).
30. P. Murphy, S. Mukerjee, J. Moore, *Phys. Rev. B* **78**, 161406 (2008).





31. J. Koch, M.E. Raikh and F von Oppen, *Phys. Rev. Lett.* **96**, 056803 (2006).
32. Karol Izydor Wysokiński, *Phys. Rev. B* **82**, 115423 (2010).
33. B. Szukiewicz, K.I. Wysokiński, in preparation
34. S.D. Franceschi, L. Kouwenhoven, C. Schönenberger and W. Wernsdorfer, *Nature Nanotechnology* **5**, 703 (2010).
35. P. Machon, M. Eschrig and W. Belzig, *Phys. Rev. Lett.* **110**, 047002 (2013).
36. M.M. Wysokiński, *Acta Phys. Pol. A* **122**, 758 (2012); M.M. Wysokiński, J. Spalek, *J. Appl. Phys.* **113**, 163905 (2013).
37. C.J. Lambert and R. Raimondi, *J. Phys. Condens. Matter* **10**, 901 (1998); A. Kormanyos, I. Grace and C.J. Lambert *Phys. Rev. B* **79**, 075119 (2009).
38. C.B. Whan and T.P. Orlando, *Phys. Rev.* **B54**, R5255 (1996).
39. A. Levy Yeyati, J. C. Cuevas, A. López-Dávalos and A. Martín-Rodero, *Phys. Rev.* **B55**, R6137 (1997).
40. K. Kang, *Phys. Rev.* **B57**, 11891 (1998).
41. R. Fazio and R. Raimondi, *Phys. Rev. Lett.* **80**, 2913 (1998); *ibid.* **82**, 4950 (1999).
42. P. Schwab and R. Raimondi, *Phys. Rev.* **B59**, 1637 (1999).
43. T.I. Ivanov, *Phys. Rev.* **B59**, 169 (1999).
44. Q.F. Sun, J. Wang and T.H. Lin, *Phys. Rev. B* **59** 3831 (1999); *Phys. Rev. B* **62**, 648 (2000); Y. Zhu, T.H. Lin and Q.F. Sun, *Phys. Rev. B* **69**, 121302 (2004).
45. M. Krawiec and K. I. Wysokiński, *Acta. Phys. Pol.* **A97**, 197 (2000).
46. A.A. Clerk, V. Ambegaokar and S. Hershfield, *Phys. Rev. B* **61**, 3555 (2000).
47. Y. Avishai, A. Golub and A. D. Zaikin, *Phys. Rev. B* **63**, 134515 (2001).
48. M. Krawiec and K.I. Wysokiński, *Supercond. Sci. Technol.* **17**, 103 (2002).
49. S.Y. Liu and X.L. Lei, *Phys. Rev. B* **70**, 205339 (2004).
50. F.S. Bergeret, A. Levy Yeyati and A. Martin-Rodero, *Phys. Rev. B* **74**, 132505 (2006); *Phys. Rev. B* **76**, 174510 (2007).
51. A. Donabidowicz, T. Domański, K.I. Wysokiński, *Acta Phys. Polonica A* **112**, 157 (2007); A. Donabidowicz and T. Domański, *Acta Phys. Polonica A* **114**, 75 (2008); T. Domański and A. Donabidowicz, *Phys. Rev. B* **78** 073105 (2008); T. Domański, A. Donabidowicz and K.I. Wysokiński, *Phys. Rev. B* **78** 144515 (2008); J. Barański and T. Domański, *Phys. Rev. B* **84** 195424 (2011).

52. P. Trocha and J. Barnaś, *Phys. Rev. B* **85**, 085408 (2012); R. Świrkowicz, M. Wierzbicki and J. Barnaś, *Phys. Rev. B* **80**, 195409 (2009); M. Wierzbicki and R. Swirkowicz, *Phys. Rev. B* **84**, 075410 (2011); M. Wierzbicki and R. Świrkowicz, *Phys. Rev. B* **82**, 165334 (2010).
53. H.J. Xue, T.Q. Lü, H.C. Zhang, H.T. Yin, L. Cui and Z.L. He, *Chin. Phys.* B **20**, 027301 (2011); *ibid* **21**, 037201 (2012).
54. B.M. Andersen, K. Flensberg, V. Koerting and J. Paaske, *Phys. Rev. Lett.* **107**, 256802 (2011); V. Koerting, B.M. Andersen, K. Flensberg and J. Paaske, *Phys. Rev. B* **82**, 245108 (2010).
55. M. Tsaousidou and G.P. Triberis, *J. Phys.: Condens. Matter* **22** 355304 (2010); J. Azema, A.M. Dare, S. Schäfer and P. Lombardo, `arXiv:1204:5360`; P. Castelanos, R. Franco, J. Silva-Valencia and M.S. Figueira, *J. Supercond. Nov. Magn.* **23**, 153 (2010).
56. M.R. Buitelaar, T. Nussbaumer and C. Schönenberger, *Phys. Rev. Lett.* **89**, 256801 (2002); M.R. Buitelaar, W. Belzig, T. Nussbaumer, B. Babić, C. Bruder and C. Schönenberger, *Phys. Rev. Lett.* **91**, 057005 (2003).
57. J.-P. Cleuziou, W. Wernsdorfer, V. Bouchiat, T. Ondarçuhu and M. Monthioux, *Nature Nanotechnology* **1**, 53 (2006).
58. P. Jarillo-Herrero, J. A. van Dam, L. P. Kouwenhoven, Nature **439**, 953 (2006); J. A. van Dam, Y. V. Nazarov, E. P. A. M. Bakkers, S. De Franceschi and L. P. Kouwenhoven, *Nature* **442**, 667 (2006).
59. H.I. Jorgensen, K. Grove-Rasmussen, T. Novotný, K. Flensberg, P.E. Lindelof, *Phys. Rev. Lett.* **96**, 207003 (2006); K. Grove-Rasmussen, H.I. Jorgensen and P. E. Lindelof, *New J. Phys.* **9** 124 (2007); H.I. Jørgensen, T. Novotný, K. Grove-Rasmussen, K. Flensberg and P.E. Lindelof, *Nano Lett.* **7**, 2441 (2007).
60. A. Eichler, M. Weiss, S. Oberholzer, C. Schönenberger, A. Levy Yeyati, J. C. Cuevas and A. Martín-Rodero, *Phys. Rev. Lett.* **99**, 126602 (2007); A. Eichler, R. Deblock, M. Weiss, C. Karrasch, V. Meden, C. Schönenberger and H. Bouchiat, *Phys. Rev. B* **79**, 161407 (2009); L. Hofstetter, S. Csonka, J. Nygård and C. Schönenberger, *Nature* **461**, 960 (2009); L. G. Herrmann, F. Portier, P. Roche, A.L. Yeyati, T. Kontos and C. Strunk, *Phys. Rev. Lett.* **104**, 026801 (2010).
61. T. Sand-Jespersen, J. Paaske, B.M. Andersen, K. Grove-Rasmussen, H.I. Jørgensen, M. Aagesen, C. B. Sørensen, P. E. Lindelof, K. Flensberg and J. Nygård, *Phys. Rev. Lett.* **99**, 126603 (2007).



62. R.S. Deacon, Y. Tanaka, A. Oiwa, R. Sakano, K. Yoshida, K. Shibata, K. Hirakawa and S. Tarucha, *Phys. Rev. Lett.* **104**, 076805 (2010); *Phys. Rev. B* **81**, 121308 (2010).
63. J.D. Pillet, C.H.L. Quay, P. Morfin, C. Bena, A.L. Yeyati and P. Joez, *Nature Physics* **6**, 965 (2010).
64. M. Meschke, J.T. Peltonen, J.P. Pekola and F. Giazotto *Phys. Rev. B* **84**, 214514 (2011).
65. A. Martin-Rodero, A. Levy Yeyati, *Advances in Physics* **60**, 899 (2011).
66. G. Michałek, B.R. Bułka, T. Domański and K.I. Wysokiński, *Phys. Rev. B* **88**, 155425 (2013).
67. F. Mazza, R. Bosisio, G. Benenti, V. Giovannetti, R. Fazio and F. Taddei, *New J. Phys.* **16**, 085001 (2014).

*Lecture Notes of the 11th International School on Theoretical Physics*

# *Symmetry, Spin Dynamics and the Properties of Nanostructures*

***Symmetry and Structural Properties of Condensed Matter***

***Rzeszów, Poland***
***1 – 6 September 2014***

*Editors*

**Vitalii Dugaev**

**Andrzej Wal**

**Józef Barnaś**

World Scientific

NEW JERSEY · LONDON · SINGAPORE · BEIJING · SHANGHAI · HONG KONG · TAIPEI · CHENNAI · TOKYO